Journal of Power Sources 239 (2013) 175–180

Contents lists available at SciVerse ScienceDirect

Journal of Power Sources

journal homepage: www.elsevier.com/locate/jpowsour

In-situ Fourier transform infrared spectroscopic analysis on dynamic behavior of electrolyte solution on $LiFePO_4$ cathode

Yasuhiro Akita, Midori Segawa, Hirokazu Munakata, Kiyoshi Kanamura*

Department of Applied Chemistry, Graduate School of Urban Environmental Sciences, Tokyo Metropolitan University, 1-1 Minami-Ohsawa, Hachioji, Tokyo 192-0397, Japan

HIGHLIGHTS

- Dynamic behavior of electrolyte solution on $LiFePO_4$ was performed by *in-situ* FT-IR.
- Solvation/desolvation of Li^+ on $LiFePO_4$ was observed during the charge and discharge.
- No decomposition of electrolyte solution was observed even at 4.3 V vs. Li/Li^+.
- The electrolyte solution was decomposed at 4.5 V vs. Li/Li^+ with CO_2 evolution.

GRAPHICAL ABSTRACT

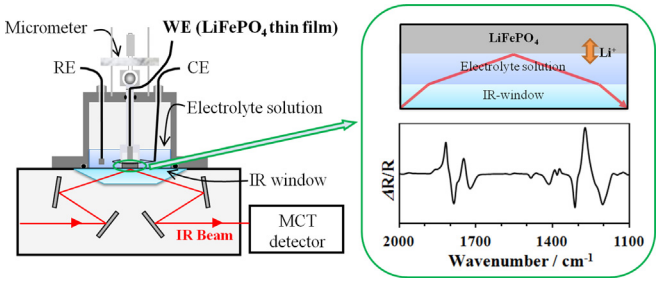

ARTICLE INFO

Article history:
Received 11 January 2013
Received in revised form
18 March 2013
Accepted 23 March 2013
Available online 3 April 2013

Keywords:
Lithium-ion battery
Lithium iron phosphate
In-situ Fourier transform infrared spectroscopy
Thin film electrode
Decomposition product

ABSTRACT

The dynamic behavior of 1.0 mol dm^{-3} $LiPF_6$ in ethylene carbonate (EC) and diethyl carbonate (DEC) mixed solvent (1:1 in volume) on lithium iron phosphate ($LiFePO_4$) thin film electrode fabricated by RF-sputtering was investigated by *in-situ* Fourier transform infrared (FT-IR) spectroscopy. The solvation and desolvation reactions of EC and DEC with Li^+ ion were observed in the charge and discharge processes of thin film electrode, respectively. In addition, the adsorption of solvent molecules on the electrode surface was suggested by polarized IR analyses. Lithium alkylcarbonate, lithium carboxylate and lithium carbonate were formed as decomposition products of the electrolyte solution at the anodic potential more than 4.5 V vs. Li/Li^+.

1. Introduction

Lithium ion batteries are promising candidates for an electric power source of hybrid electric vehicles (HEV) and electric vehicles (EV). The organic solvents with Li-salt used as electrolyte solutions are decomposed both on cathode and anode [1–4]. The decomposition products formed on the electrode surface are called "solid electrolyte interface (SEI)", which suppresses further decomposition of the electrolyte solution. It has been found to play an important role in stabilizing battery operations. There have been several reports on the oxidation reactions of electrolyte solutions on the cathode such as $LiCoO_2$, $LiMn_2O_4$, $LiNi_{0.8}Co_{0.2}O_2$, $LiNi_{0.8}Co_{0.15}Al_{0.05}O_2$ and $LiFePO_4$ [5–10]. It was found that the oxidation reactions lead to the degradation of cycle performance. Among them, $LiFePO_4$ is considered as one of the promising cathode materials for lithium ion batteries due to low cost, low toxicity, high

* Corresponding author. Tel./fax: +81 42 677 2828.
E-mail address: kanamura@tmu.ac.jp (K. Kanamura).

0378-7753/$ – see front matter © 2013 Elsevier B.V. All rights reserved.
http://dx.doi.org/10.1016/j.jpowsour.2013.03.134

thermal stability and high safety [11–14]. Recently, it is used also as a coating material to improve electrochemical performances of other cathode materials. For example, it was reported by Wang et al. that $LiFePO_4$ coating is effective to improve the thermal stability and electrochemical performance of $LiCoO_2$ at high temperatures [15]. However, the reason why the cathode surface is stabilized by $LiFePO_4$ coating is not still clear.

So far, we have investigated the decomposition behaviors of various electrolyte solutions on $LiCoO_2$ thin film electrode by *in-situ* FT-IR measurements [16–21], in which it was found that electrolyte solutions decomposed on $LiCoO_2$ thin film electrode during the charge process at more than 3.9 V vs. Li/Li^+ [20,21]. In this paper, we applied *in-situ* FT-IR technique to investigate the dynamic behavior of 1.0 mol dm^{-3} $LiPF_6$ in ethylene carbonate (EC) and diethyl carbonate (DEC) mixed solvent (1:1 in volume) on $LiFePO_4$ thin film electrode, and compared it with that on $LiCoO_2$.

2. Experimental

2.1. Preparation of $LiFePO_4$ thin film electrode

Carbon-coated $LiFePO_4$ ($LiFePO_4$/C) powder for the target used in RF-sputtering was hydrothermally synthesized according to our previous study [22]. Li_3PO_4, $FeSO_4 \cdot 7H_2O$ and carboxymethyl cellulose sodium salt in H_2O were used as raw materials for the preparation of $LiFePO_4$/C. The raw materials were hydrothermally treated under stirring at 200 °C for 2 h and gray-colored powder was obtained. This powder was then converted to $LiFePO_4$/C via heat treatment at 700 °C in Ar/H_2 (97/3 in vol.). $LiFePO_4$ thin film was fabricated on Au disk by RF-sputtering (TOKKI, SPK301). The following deposition conditions were employed: introduced gas in camber = Ar/H_2 (97/3), working pressure = 2.0×10^{-2} Torr, RF-power = 70 W, sputtering duration = 2 h. After the sputtering, the as-prepared film was heated at 650 °C in Ar/H_2 (97/3 in vol.) to improve the crystallinity of $LiFePO_4$. The crystal structures of films were characterized by X-ray diffraction (XRD, RINT 2000/PC, Rigaku) and Raman spectroscopy (NRS-1000, JASCO). The surface morphology and thickness of films were observed by scanning electron microscopy (SEM, JSM-6490A, JEOL), in which $LiFePO_4$ thin film was formed on Au-coated quartz plate.

2.2. In-situ FT-IR measurement

In-situ FT-IR measurement cell was constructed in three-electrode system (Fig. 1). Reflection spectra of samples were collected using FT-IR spectrometer (FT/IR-670, JASCO) with a mercury cadmium telluride (MCT) detector. A trapezoidal CaF_2 crystal with a measurable frequency range of more than 1100 cm^{-1} was used as an IR window. The prepared $LiFePO_4$ thin film electrode as a working electrode was placed on the IR window. A nickel wire was used as a counter electrode, and lithium metal was used as a reference electrode. 1.0 mol dm^{-3} $LiPF_6$ in EC and DEC mixed solvent (1:1 in vol.) was used as an electrolyte solution. *In-situ* FT-IR measurements were performed with *p*- and *s*-polarized IR beams in order to investigate the states of electrolyte solution on the electrode surface and in bulk, respectively. The IR measurement with non-polarized IR beam was also performed to confirm the validity of spectra obtained using *p*- and *s*-polarized IR beams, by comparison among *p*-, *s*- and non-polarized spectra since the absorption peaks in *p*-, *s*-polarized ones separately appear in the non-polarized one. The charge–discharge tests were performed by cyclic voltammetry in a potential range from 2.9 V to 4.3 V vs. Li/Li^+ at a scan rate of 20 mV min^{-1} by using a potentiostat (HSV-100, Hokuto denko). The reflectance spectra were collected with 100 mV intervals during the potential sweep. The interferogram and resolution of FT-IR measurements were set to be 200 and 4 cm^{-1}, respectively. For further investigation on the oxidative behavior of electrolyte solution, *in-situ* FT-IR measurements at high electrode potentials were also carried out. In those, the electrode potential was swept from the open circuit potential (OCP) of to 6.0 V vs. Li/Li^+ at a scan rate of 5 mV min^{-1} using a potentiostat (PARSTAT 2263, Princeton Applied Research) and the IR beam was *p*-polarized.

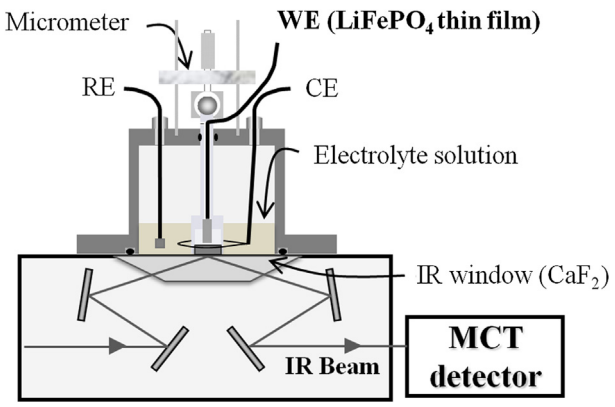

Fig. 1. Schematic illustration of *in-situ* FT-IR measurement cell.

To clarify the difference between two reflectance spectra, a subtractively normalized interfacial FT-IR (SNIFT-IR) was calculated according to the following Equation (1):

$$\Delta R/R = (R_1 - R_0)/R_0 \quad (1)$$

where R_0 is reflectance spectrum obtained at an arbitrary electrode potential and R_1 is that obtained at a different electrode potential. In this spectrum, upward and downward bands correspond to the decrease and increase in chemical bond, respectively. According to the reports by Ikezawa et al. [23,24], the difference between free and Li^+-solvating solvent molecules was estimated by comparing the spectra for EC + DEC (1:1 in vol.) mixture with and without $LiPF_6$, which were measured using a single reflectance attenuated total reflection (ATR) attachment. The FT-IR measurements for EC and DEC were also performed separately for the assignments of those molecules in EC + DEC mixed solvent.

3. Results and discussion

3.1. Characterization of $LiFePO_4$ thin film electrode

Fig. 2 shows the results of XRD measurements. The XRD pattern of $LiFePO_4$ thin film on Au substrate was in good agreement with that of the target powder used for RF-sputtering. However, the main peak for $LiFePO_4$ thin film appeared at $2\theta = \sim 21°$ although the target powder had the strongest peak at $2\theta = \sim 36°$. Therefore, it is considered for the thin film that the *b*-axis of olivine is parallel to Au substrate. Fig. 3 shows Raman spectra of the target powder and $LiFePO_4$ thin film electrode. The Raman shifts at 947 and 992 cm^{-1} are attributed to $LiFePO_4$, and those at 1350 and 1600 cm^{-1} are corresponding to D-band and G-band of the carbon coating on $LiFePO_4$. The SEM images of $LiFePO_4$ thin film are shown in Fig. 4. The surface morphology of thin film was flat enough for using in FT-IR measurements by external reflection method, and its thickness was about 700 nm. Fig. 5 shows the cyclic voltammogram for $LiFePO_4$ thin film electrode in 1.0 mol dm^{-3} $LiPF_6$/EC + DEC (1:1 in vol.). Li^+ extraction and insertion were confirmed at 3.6 V vs. Li/Li^+ in charge process and 3.3 V vs. Li/Li^+ in discharging one,

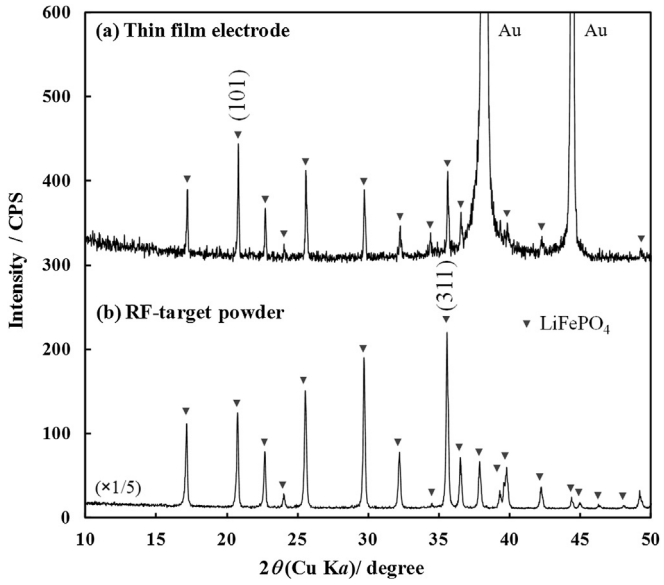

Fig. 2. XRD patterns of (a) $LiFePO_4$ thin film electrode prepared by RF-sputtering and (b) $LiFePO_4$/C target powder.

respectively. On assumption that the thin film electrode is composed of a $LiFePO_4$ single crystal, the first charge and discharge capacities are estimated to be 55 and 53 mA h g^{-1}, respectively. However, the actual capacities are expected to be higher since the prepared thin film is not a single crystal and includes some amount of carbon.

3.2. IR absorption of free and Li^+-solvating solvent molecules

The IR-absorption spectra for EC, DEC and their mixture (1:1 in volume) were shown in Fig. 6, respectively. EC showed strong peaks at 1799 and 1773 cm^{-1} corresponding to C═O stretching vibrations, 1482 cm^{-1} corresponding to the scissoring vibration of CH_2, 1389 cm^{-1} corresponding to wagging vibration of CH_2, 1151 and 1068 cm^{-1} corresponding to C–O stretching vibrations [24]. Similarly, DEC showed strong peaks at 1736, 1470, 1374 and 1255 cm^{-1}. Those peaks observed for EC and DEC were respectively confirmed

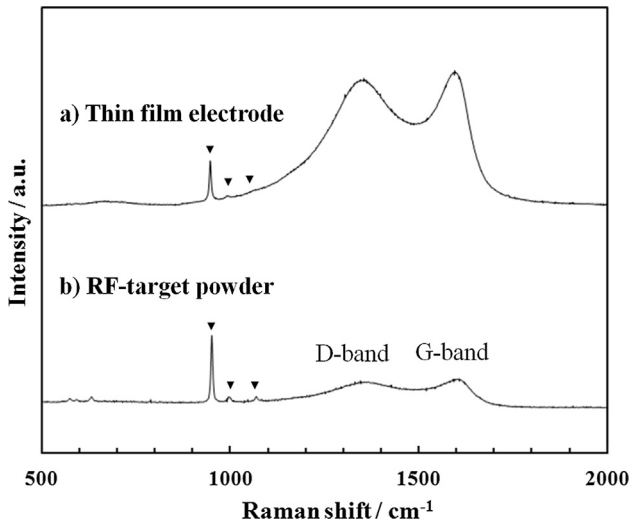

Fig. 3. Raman spectra for (a) $LiFePO_4$ thin film electrode prepared by RF-sputtering and (b) $LiFePO_4$/C target powder.

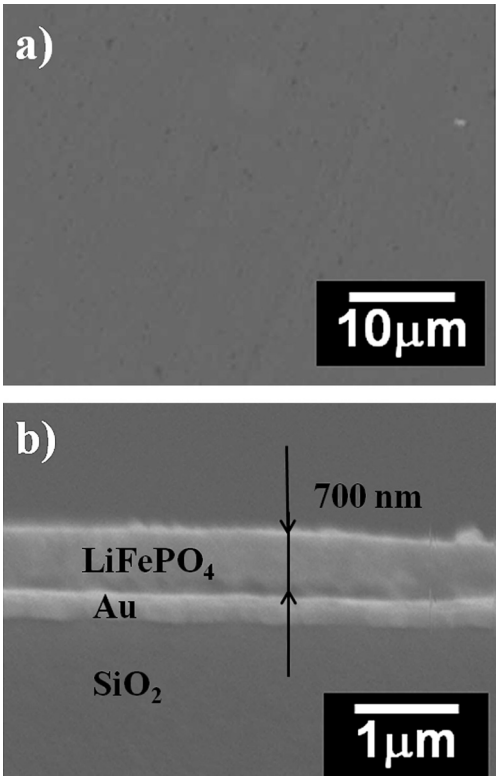

Fig. 4. SEM images of (a) surface and (b) cross-section of $LiFePO_4$ thin film electrode prepared by RF-sputtering on an Au-coated quart glass.

for EC + DEC (1:1) mixture, and its spectrum accorded with the sum of EC and DEC spectra. A series of absorption spectra for EC + DEC (1:1) with different $LiPF_6$ concentrations were shown in Fig. 7. To clarify the difference in those spectra, the differential spectra were also calculated against that for EC + DEC (1:1) without $LiPF_6$. In the differential spectra, upward peaks were assigned to free solvent molecules, and downward ones were assigned to Li^+-solvating molecules. The assignments were summarized in Table 1. In the case of Li^+-solvating EC, the wavenumber of C═O stretching vibration shifted to lower wavenumber than that of pristine EC. On the contrary, the C–O stretching vibration showed the opposite behavior, namely the wavenumber shifted to higher value. According to the previous study reported by Li et al. [25], Li^+ is

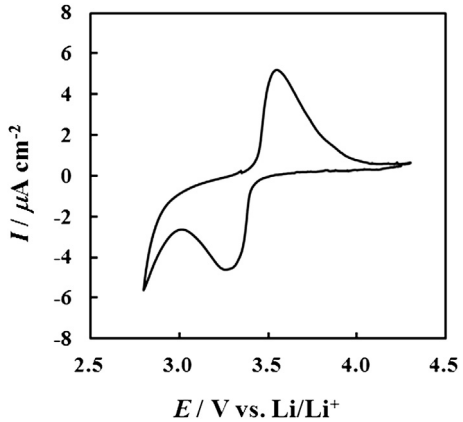

Fig. 5. Cyclic voltammogram for $LiFePO_4$ thin film electrode in 1.0 mol dm^{-3} $LiPF_6$/EC + DEC (1:1) measured using *in-situ* FI-IR cell at a scan rate of 20 mV min^{-1}.

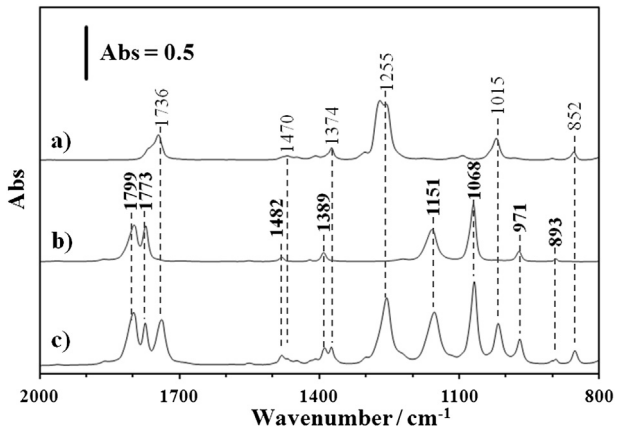

Fig. 6. FT-IR spectra for (a) DEC, (b) EC and (c) EC + DEC (1:1) mixture without $LiPF_6$ electrolyte.

solvated with EC and forms C═O···Li^+ coordination bond. Consequently, the C═O (1764 and 1715 cm^{-1}) bond is weakened and C–O bond (1197 and 1302 cm^{-1}) is formed. It is worthy noted that no shift was observed for those peaks when the $LiPF_6$ concentration changed. Therefore, it is suggested that the state and conformation of Li^+-solvating EC and DEC are maintained in the $LiPF_6$ concentration from 0 to 1.0 mol dm^{-3}.

3.3. Dynamic behavior of electrolyte solution on $LiFePO_4$ thin film electrode

Fig. 8 shows the *in-situ* SNIFT-IR spectra for 1.0 mol dm^{-3} $LiPF_6$/EC + DEC (1:1) on $LiFePO_4$ thin film electrode during charge–discharge tests, collected using: (a) *p*-polarized, (b) *s*-polarized and (c) non-polarized IR beams. During the charge process of $LiFePO_4$ (anodic potential sweep), upward peaks were observed at 1822, 1747 and 1273 cm^{-1}, which correspond to free EC and DEC. This behavior is due to the decrease of free EC and DEC molecules on the surface of $LiFePO_4$ thin film electrode. At the same time, downward peaks at 1784, 1720 and 1313 cm^{-1} were observed. They correspond to the formation of Li^+-solvating EC and DEC molecules. Therefore, it is suggested that Li^+-solvating EC and DEC increase along with the decrease of free EC and DEC on $LiFePO_4$ during charge process. On the contrary, the desolvation reaction of Li^+ was observed during the discharge process, in which Li^+ insertion to $FePO_4$ occurs. The Li^+ solvation observed even during the electrode potential sweep from 4.3 to

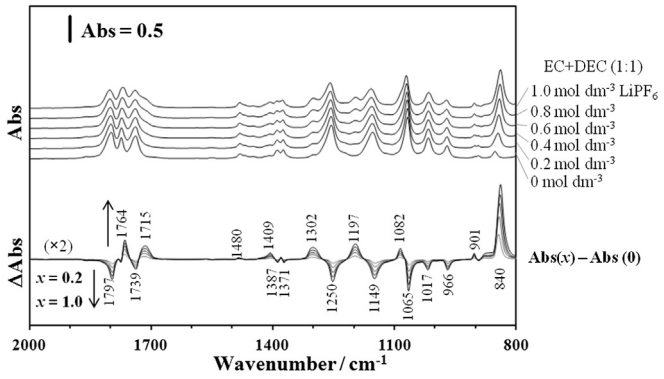

Fig. 7. IR adsorption spectra for EC + DEC (1:1) mixture with different $LiPF_6$ concentrations (0–1.0 mol dm^{-3}), and the differential absorption spectra (ΔAbs) calculated for each $LiPF_6$ concentration (x mol dm^{-3}, x = 0.2–1.0) against that without $LiPF_6$.

Table 1
Peak assignments for the differential spectra of EC + DEC (1:1) system.

Wavenumber [cm^{-1}]	Molecule state		Vibration mode
	Free	Li^+-solvating	
1797	EC	–	C═O stretching
1764	–	EC	C═O stretching
1739	DEC	–	C═O stretching
1715	–	DEC	C═O stretching
1480	EC and DEC	–	C–H wagging
1409	EC and DEC	–	C–H wagging
1387	DEC	DEC	C–H scissoring
1371	EC	EC	C–H scissoring
1302	–	DEC	C–O stretching
1250	DEC	–	C–O stretching
1197	–	EC	C–O stretching
1149	EC	–	C–O stretching
1082	–	EC	C–O stretching
1065	EC	–	C–O stretching
1017	DEC	DEC	C–C stretching
966	EC	EC	C–C stretching

3.9 V is due to the delay in the interfacial behavior between the electrolyte solution and $LiFePO_4$ thin film electrode since the sweep rate of electrode potential was relatively fast. Except of this difference, the spectral changes during the discharge process were reverse of those in the anodic process. Consequently, no peak corresponding to the decomposition of 1.0 mol dm^{-3} $LiPF_6$/EC + DEC (1:1) was observed in both charge and discharge processes, suggesting that SEI formation hardly occurs on $LiFePO_4$ in a potential range from 2.9 V to 4.3 V vs. Li/Li^+. This stable surface on $LiFePO_4$ is expected to relate with the following result. In the spectra measured using *p*-polarized IR beam, the peaks attributable to C═O and C–O vibrations of Li^+-solvating EC and DEC shifted about 20 cm^{-1} toward high wavenumber compared with those observed in the differential spectra shown in Fig. 7. However, such peak shift was hardly observed for the wagging vibration of CH_2. This behavior shows the adsorption of free EC and DEC onto the electrode via carbonate groups.

The dynamic behaviors of EC and DEC on $LiFePO_4$ were analyzed also using *s*-polarized IR beam (Fig. 8(b)), which provides information on their behavior in electrolyte solution bulk. The downward peaks (1764, 1708, 1296 and 1194 cm^{-1}) corresponding to Li^+-solvating EC and DEC were observed, and upward ones (1799, 1739, 1254 and 1152 cm^{-1}) for free EC and DEC were also confirmed in the course of electrode potential sweep from OCP to 4.3 V vs. Li/Li^+. The wavenumbers of free and Li^+-solvating molecules were in good agreement with those in Table 1. This result indicates that the solvating EC and DEC diffuses from the electrode surface to electrolyte solution bulk during the charge process. On the contrary, the diffusions of free EC and DEC from the electrode surface to electrolyte solution bulk were confirmed in the discharge process, in which the free and Li^+-solvating molecules appeared as downward and upward peaks, respectively. In addition, the *s*-polarized spectra showed no decomposition peak of electrolyte solution as the same as *p*-polarized ones.

When non-polarized IR beam was applied, the resulting SNIFT-IR spectra (Fig. 8(c)) showed both characteristics observed by using *p*- (interfacial behavior) and *s*-polarized (bulk behavior) IR beams. This supports the validity of *in-situ* FT-IR measurements performed in this study.

The SNIFT-IR spectra obtained at high electrode potentials (4.3–6.0 V vs. Li/Li^+) are shown in Fig. 9. The downward peak attributable to CO_2 was observed at 2339 cm^{-1}. In addition, the upward peaks for free EC and DEC were slightly observed during the potential sweep from 4.3 to 4.5 V Li/Li^+. Since $LiFePO_4$ is

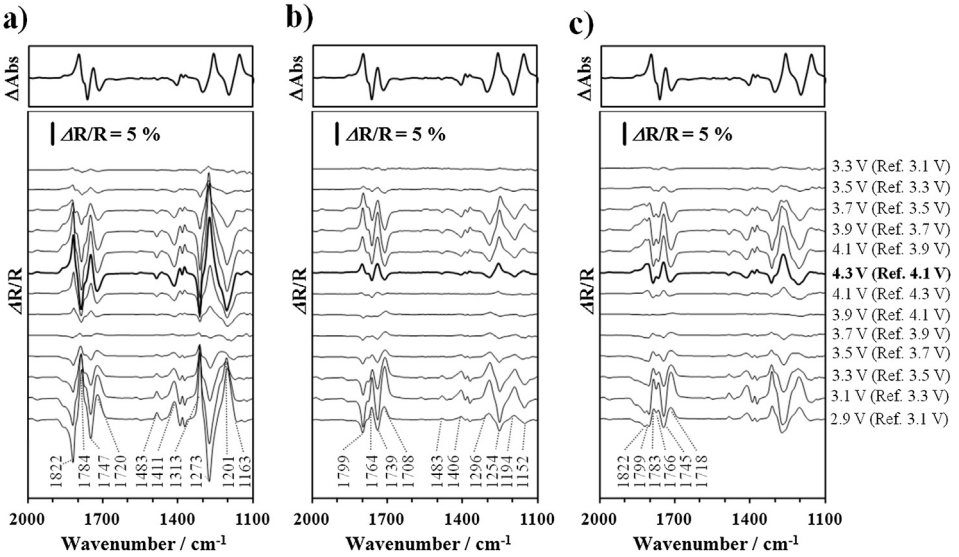

Fig. 8. *In-situ* SNIFT-IR spectra for 1.0 mol dm^{-3} $LiPF_6$/EC + DEC (1:1) on $LiFePO_4$ thin film electrode, measured in a potential range from 2.9 V to 4.3 V vs. Li/Li^+ at a scan rate of 20 mV min^{-1} using (a) *p*-polarized, (b) *s*-polarized and (c) non-polarized IR beams. Upward and downward peaks in each ΔAbs spectrum (differential spectrum between EC + DEC (1:1) with 0 and 1.0 mol dm^{-3} $LiPF_6$ concentrations) correspond to and Li^+-solvating solvent molecules, respectively.

completely converted to $FePO_4$ at those high electrode potentials by Li^+ extraction during charge process, the upward peaks are due to not Li^+ solvation reaction but the decomposition of electrolyte solution. Actually, the downward peaks, which were not assigned to free and Li^+-solvating EC and DEC, were clearly observed at more anodic potentials than 4.8 V vs. Li/Li^+. According to the previous report [26], those downward peaks are assignable as follows: 1680 and 1630 cm^{-1} = lithium alkylcarbonate (ROCOOLi), 1558 cm^{-1} = lithium carboxylate (RCOOLi) and 1506 cm^{-1} = Li_2CO_3. Form these results, it can be said that the oxidative decomposition of 1.0 mol dm^{-3} $LiPF_6$/EC + DEC (1:1) occurs on $LiFePO_4$ at about 4.5 V vs. Li/Li^+. As considering that the oxidative decomposition of electrolyte solution occurs on $LiCoO_2$ at approximately 4 V vs. Li/Li^+ [19–21], it can be expected that the activity of $LiFePO_4$ on electrolyte decomposition is very low. From this viewpoint, $LiFePO_4$ is promising to improve the safety of lithium-ion batteries as a coating material for cathode materials.

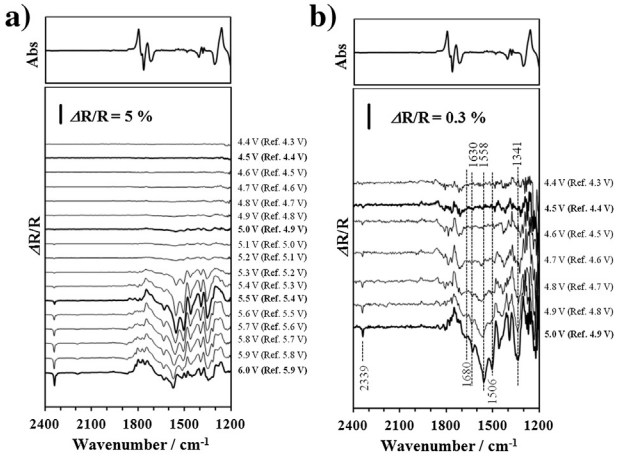

Fig. 9. (a) *In-situ* SNIFT-IR spectra for 1.0 mol dm^{-3} $LiPF_6$/EC + DEC (1:1) on $LiFePO_4$ thin film electrode, measured in a potential range from OCP to 6.0 V vs. Li/Li^+ at a scan rate of 5 mV min^{-1} using *p*-polarized IR-beam and (b) the magnified spectra from 4.3 to 5.0 V vs. Li/Li^+.

4. Conclusions

In-situ FT-IR measurements on 1.0 mol dm^{-3} $LiPF_6$/EC + DEC (1:1) on the $LiFePO_4$ thin film electrode fabricated by RF-sputtering were performed. The solvation and desolvation behaviors of EC and DEC with Li^+ ion on the $LiFePO_4$ electrode were observed during the charge and discharging processes. No decomposition of electrolyte solution was observed even at 4.3 V vs. Li/Li^+. However, when the electrode potential reached to 4.5 V vs. Li/Li^+, the electrolyte solution was decomposed to form ROCOOLi, RCOOLi and Li_2CO_3 with CO_2 evolution. This electrode potential is very high compared with that on $LiCoO_2$ (approximately 4 V vs. Li/Li^+), suggesting that the activity of $LiFePO_4$ on electrolyte decomposition is very low.

References

[1] J.B. Goodenough, Y. Kim, Chem. Mater. 22 (2010) 587–603.
[2] E. Peled, C. Menachem, D. Bar-Tow, A. Melman, J. Electrochem. Soc. 143 (1996) L4–L7.
[3] X. Zhang, R. Kostecki, T.J. Richardson, J.K. Pugh, P.N. Ross Jr., J. Electrochem. Soc. 148 (2001) A1341–A1345.
[4] K. Xu, Chem. Rev. 104 (2004) 4303–4417.
[5] W. Li, B.L. Lucht, J. Electrochem. Soc. 153 (2006) A1617–A1625.
[6] D. Ostrovskii, F. Ronci, B. Scrosati, P. Jacobsson, J. Power Sources 103 (2001) 10–17.
[7] R. Sharabi, E. Markevich, V. Borgel, G. Salitra, D. Aurbach, G. Semrau, M.A. Schmidt, Electrochem. Solid-State Lett. 13 (2010) A32–A35.
[8] N. Dupré, J.F. Martin, J. Oliveri, P. Soudan, A. Yamada, R. Kanno, D. Guyomard, J. Power Sources 196 (2011) 4791–4800.
[9] D. Aurbach, B. Markovsky, A. Rodkin, E. Levi, Y.S. Cohen, H.J. Kim, M. Schmidt, Electrochim. Acta 47 (2002) 4291–4306.
[10] D. Aurbach, B. Markovsky, G. Salitra, E. Markevich, Y. Talyossef, M. Koltypin, L. Nazar, B. Ellis, D. Kovacheva, J. Power Sources 165 (2007) 491–499.
[11] M. Li, L. Sun, K. Sun, S. Yu, R. Wang, H. Xie, J. Solid State Electrochem. 16 (2012) 3581–3586.
[12] G. Arnold, J. Garche, R. Hemmer, S. Ströbele, C. Vogler, M.W. Mehrens, J. Power Sources 119–121 (2003) 247–251.
[13] K. Zaghib, J. Dubé, A. Dallaire, K. Galoustov, A. Guerfi, M. Ramanathan, A. Benmayza, J. Prakash, A. Mauger, C.M. Julien, J. Power Sources 219 (2012) 36–44.
[14] A.K. Padhi, K.S. Nanjundaswamy, J.B. Goodenough, J. Electrochem. Soc. 144 (1997) 1188–1194.
[15] H. Wang, W.D. Zhang, L.Y. Zhu, M.C. Chen, Solid State Ionics 178 (2007) 131–136.
[16] K. Kanamura, T. Okagawa, Z. Takehara, J. Power Sources 57 (1995) 119–123.
[17] K. Kanamura, S. Toriyama, S. Shiraishi, M. Ohashi, Z. Takehara, J. Electroanal. Chem. 419 (1996) 77–84.

[18] K. Kanamura, T. Umegaki, M. Ohashi, S. Toriyama, S. Shiraishi, Z. Takehara, Electrochim. Acta 47 (2001) 433–439.
[19] T. Matsushita, K. Dokko, K. Kanamura, J. Power Sources 146 (2005) 360–364.
[20] M. Matsui, K. Dokko, K. Kanamura, J. Power Sources 177 (2008) 184–193.
[21] M. Matsui, K. Dokko, Y. Akita, H. Munakata, K. Kanamura, J. Power Sources 210 (2012) 60–66.
[22] H. Nakano, K. Dokko, S. Koizumi, H. Tannai, K. Kanamura, J. Electrochem. Soc. 155 (2008) A909–A914.
[23] Y. Ikezawa, T. Ariga, Electrochim. Acta 52 (2007) 2710–2715.
[24] Y. Ikezawa, H. Nishi, Electrochim. Acta 53 (2008) 3663–3669.
[25] J.T. Li, S.R. Chen, F.S. Ke, G.Z. Wei, L. Huang, S.G. Sun, J. Electroanal. Chem. 649 (2010) 171–176.
[26] P. Verma, P. Maire, P. Novák, Electrochim. Acta 55 (2010) 6332–6341.